

Evaluation of modeled cloud properties against aircraft observations for air quality applications

Junhua Zhang,¹ Wanmin Gong,¹ W. Richard Leitch,¹ and J. Walter Strapp¹

Received 30 May 2006; revised 12 October 2006; accepted 17 January 2007; published 26 April 2007.

[1] Cloud microphysical properties are critical for simulating cloud processing of gases and aerosols in air quality models. In this study, cloud liquid water contents (LWC) predicted from a meteorological model at two horizontal resolutions (15 and 2.5 km) are evaluated against aircraft observations during the 2004 International Consortium for Atmospheric Research on Transport and Transformation (ICARTT) campaign. A point-by-point comparison along flight tracks shows good model-observation correlation for temperature and humidity but poor correlation for LWC due to the mismatch in timing and positioning of the clouds between model simulations and observations. Thus a statistical approach is used to compare properties of modeled and observed clouds over the flight domain. The model captures the observed vertical variation of LWC for the towering cumulus (TCu) cases and reproduces the observed variation of LWC from flight to flight independent of cloud types. The model is able to distinguish the difference in the mean and standard deviation of LWC between stratocumulus (SCu) and TCu. However, the “in-cloud” LWC values were generally overpredicted by the model at both resolutions. For SCu, the overprediction is 99% and 45% for the 15- and 2.5-km resolution simulations, respectively, while the overprediction for TCu is slightly smaller at 74% for the 15-km resolution and 24% for the 2.5-km resolution model simulations. The SCu observations were scaled up to enable comparisons at the model-grid scales for these flights. This comparison also shows overpredictions of LWC by the model, although the overprediction is smaller for the model at 15-km resolution.

Citation: Zhang, J., W. Gong, W. R. Leitch, and J. W. Strapp (2007), Evaluation of modeled cloud properties against aircraft observations for air quality applications, *J. Geophys. Res.*, 112, D10S16, doi:10.1029/2006JD007596.

1. Introduction

[2] Clouds play an important role in the processing and cycling of chemicals in the atmosphere. Once trace gases and aerosols enter cloud droplets, they can dissolve, dissociate and undergo chemical reactions [Seinfeld and Pandis, 1998]. For example, it is estimated that up to 80% of the total global production of sulphate and about 50% of the global sulphate burden is contributed by aqueous phase oxidation in the clouds [Barth et al., 2000; Rasch et al., 2000]. Wet deposition resulting from precipitation formed in clouds is one of the most efficient sinks for aerosols and other soluble tracers. Clouds also redistribute trace gases and aerosol particles. Updrafts in convective clouds transport trace gases from the generally more polluted lower levels to cleaner higher levels where ozone and particle production may be more efficient [e.g., Renard et al., 1994; Wang and Prinn, 2000; Raes and Van Dingenen, 1992; Clarke, 1993]. Representation of these physical and chemical processes in cloud is necessary for the accurate simu-

lation of the transport and transformation of trace gases and aerosol particles.

[3] Chemical transport models with representations of cloud processes at varying levels of sophistication have been used in the past to investigate the roles of clouds in processing of gases and aerosols in the atmosphere [e.g., Chang et al., 1987; Venkatram et al., 1988; Carmichael et al., 1991; Lohmann et al., 1999; Barth et al., 2000; von Salzen et al., 2000; Gong et al., 2006a]. A major challenge is the validation of the representation of cloud processes in these models. There has been a lack of suitable observations for comprehensive evaluations of in-cloud processes in air quality models. Past evaluations of modeled cloud processes have been largely done indirectly through comparisons with measurements of tracer gases and aerosols near the surface and chemical components in precipitation [e.g., Karamchandani and Venkatram, 1992; Dennis et al., 1993; McHenry and Dennis, 1994; Gong et al., 2006a].

[4] Previous air quality model evaluations indicate that the modeled cloud processing of gases and aerosols depends critically on the meteorological driver model's ability to predict cloud microphysics fields [Gong et al., 2006a, 2006b]. In-cloud sulphate production is largely driven by liquid water content; precipitation production (autoconversion) and flux have direct impact on the removal of atmospheric tracers. Therefore, in evaluating the cloud

¹Science and Technology Branch, Environment Canada, Toronto, Ontario, Canada.

chemical processing in air quality models, a major question to be addressed is how well the clouds are predicted by the meteorological driver models?

[5] In situ observations by aircraft provide valuable data sets to address this question. A number of existing studies have used in situ aircraft observations to evaluate modeled microphysical fields [e.g., *Brown and Swann*, 1997; *Reisner et al.*, 1998; *Guan et al.*, 2001, 2002; *Vaillancourt et al.*, 2003; *Garvert et al.*, 2005]. Most of the studies focused on winter clouds associated with frontal systems, usually stratiform clouds with extensive horizontal coverage. Many studies, therefore, compared model simulation with aircraft observations either in a cross section [e.g., *Reisner et al.*, 1998] or along flight tracks with different evaluation methodologies. For example, *Guan et al.* [2001, 2002] looked at hit rate (HR), false alarm rate (FAR), true skill statistic (TSS), and correlation between measured and forecasted cloud water along aircraft flight tracks, while *Vaillancourt et al.* [2003] evaluated a mixed phase cloud scheme in a weather forecast model by comparing the dynamical, thermodynamic and microphysical variables between in situ aircraft observations and the model predictions, point-by-point along 21 cloud flights. Unless the flight path is carefully designed to sample the cloud properties as demonstrated by *Garvert et al.* [2005], disparity between aircraft observation and model simulation can still be a problem even for the relative uniform winter stratiform clouds. *Reisner et al.* [1998] pointed out that the kinematic and thermodynamic characteristics of a storm need to be realistically simulated in order for the microphysical scheme to produce accurate results. A combination of aircraft and other observations, such as radar, can provide a better way to evaluate model simulations as shown in, for example, the study of *Brown and Swann* [1997], which described detailed cloud microphysical properties observed by aircraft and radar observations were used to provide vertical structure of clouds and to identify the time and location of clouds and the initial formation of precipitation.

[6] During the summer of 2004, under the coordination of the International Consortium for Atmospheric Research on Transport and Transformation (ICARTT), a large field study was conducted over eastern North America, the North Atlantic, and Western Europe to provide a better understanding of some of the issues relating to air quality and climate change [*Fehsenfeld et al.*, 2006]. As a component of the ICARTT campaign, Environment Canada, in collaboration with the National Research Council of Canada (NRCC) and Canadian Universities, conducted airborne measurements from 12 July 2004 to 18 August 2004, using the NRC-IAR (National Research Council Canada–Institute for Aerospace Research) Convair 580 aircraft. The study focused on the interactions among trace gases, aerosols and clouds, as well as the transport of pollution into the Canadian Maritimes (see K. L. Hayden et al., Cloud processing of nitrate, unpublished manuscript, 2007; A. Leithead et al., Investigation of carbonyls in cloud-water during ICARTT, unpublished manuscript, 2007). One of the study objectives was also to provide a data set for evaluating air quality models particularly on the representation of cloud processes. Along with various trace gas and aerosol measurements conducted onboard, the Convair 580 was also extensively instrumented for cloud microphysics measurements.

[7] In this paper, the performance of the Canadian Global Environmental Multiscale model (GEM [*Côté et al.*, 1998a, 1998b]) in predicting summertime cloud liquid water contents (LWC) at two horizontal resolutions (15- and 2.5-km) is examined. The GEM model at 15-km resolution is currently used as the meteorological driver model for a regional air quality model (Environment Canada's AURAMS model [*Moran et al.*, 1998]). The cloud microphysical parameters from the GEM model are used for cloud processing in AURAMS [*Gong et al.*, 2006a]. This study is a first step in an effort to evaluate cloud processing in AURAMS, and it is also a first attempt to evaluate the performance of a meteorological model in predicting cloud microphysics properties under summer continental conditions for air quality modeling purpose. Here, the model and its setup are briefly discussed in section 2. This is followed by a description of the evaluation methods and the results of the comparisons are discussed in section 3. Conclusions are given in section 4.

2. Model Description

[8] The GEM model can be configured to run either globally at a uniform resolution or with a variable resolution over the global domain and a uniform (core) mesh over an area of interest. The horizontal mesh, uniform or variable resolution, can vary from hundreds of kilometers down to single digit, and can be arbitrarily rotated [*Côté et al.*, 1998a, 1998b]. The GEM model can also be configured to run with a Limited Area Modeling (LAM) setup with the boundary conditions provided by either an objective analysis or a coarser resolution forecast model. The regional GEM model operational at the Canadian Meteorological Centre is currently configured with a variable grid with a uniform core domain centered over North America at 15-km resolution [*Mailhot et al.*, 2006].

[9] In this study, GEM with the LAM configuration at 15- and at 2.5-km horizontal resolutions each with 58 vertical levels is evaluated. The vertical levels are unevenly distributed with good resolution in the boundary layer, the upper level jet region, and the stratosphere. There are 10 levels below 850 hPa [*Mailhot et al.*, 2006]. The runs were conducted in a cascade fashion: the initial and boundary conditions for the 15-km resolution runs were obtained from the objective reanalysis data sets available at 00, 06, 12 and 18 hours, while those for the 2.5-km resolution runs were provided by the 15-km LAM forecast. Figure 1 shows the 15- and 2.5-km horizontal resolution model domains in this study.

[10] Cloud dynamical and microphysical processes are parameterized differently for the 15- and 2.5-km resolutions simulations. For the 15-km resolution, large-scale stratiform condensation process is parameterized by a Sundqvist scheme [*Sundqvist et al.*, 1989]; subgrid-scale deep convection is parameterized by a Kain-Fritsch scheme [*Kain and Fritsch*, 1990; *Kain*, 2004] which is based on a 1-D entraining/detraining plume model; and shallow convection is parameterized by a Kuo-transient scheme [*Bélair et al.*, 2005]. The Sundqvist scheme parameterizes the subgrid-scale stratiform condensation through a fractional cloud cover which, in turn, is parameterized on the basis of relative humidity at the grid scale. In the case of the 2.5-km

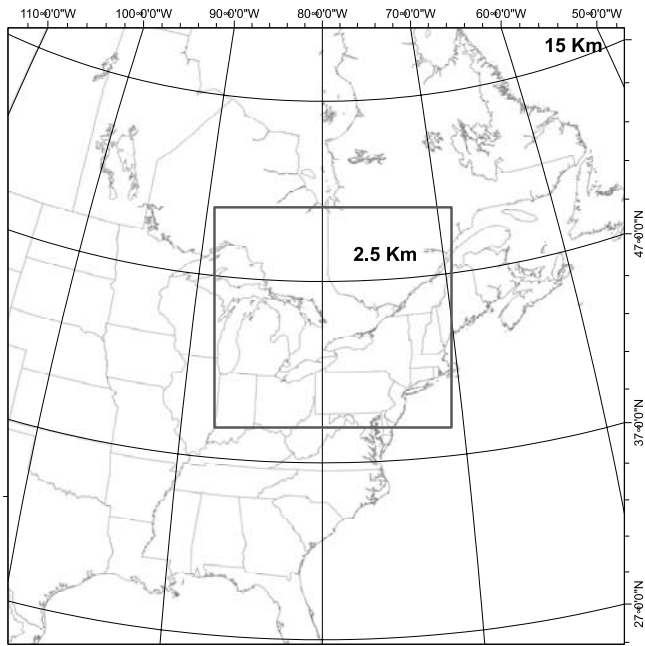


Figure 1. GEM LAM domains for the 15- and 2.5-km resolution simulations. The domain size is 3750 × 3750 km for the 15-km resolution and 1250 × 1250 km for the 2.5-km resolution.

horizontal resolution, deep convections are assumed to be resolved at this scale; cloud microphysical processes are treated explicitly by the Kong-Yau scheme [Kong and Yau, 1997]. In this scheme, condensation of vapor is parameterized by a saturation adjustment technique, in which cloud water/ice is assumed to form or evaporate depending on whether the water vapor in a grid cell is above or below the saturation value. No fractional cloud cover is considered. Cloud fraction at each model grid is either 0 or 1 depending on whether cloud water (liquid + ice) exceeds a threshold value of 0.01 g m⁻³.

3. Model Evaluation Against Observations

[11] During the ICARTT campaign, a total of 23 aircraft flights were conducted with the Canadian Convair 580 (operated by NRCC) out of Cleveland, Ohio. Not all the flights encountered significant amount of clouds. Ten of the 23 flights had sufficient cloud sampling to be used for this study. Figure 2 shows the paths of the 10 flights which are focused over the southern Great Lakes area. Clouds sampled during the campaign can be categorized into two types: stratocumulus (SCu) and towering cumulus (TCu). The TCu clouds are defined here as those cumulus that are not capped at the top of the boundary layer. They have greater vertical extent, stronger and better defined updraft cores compared to the boundary layer cumulus (or SCu). Out of the ten selected flights, five were SCu flights, which consisted mainly of several relatively long level flight legs, usually one below cloud base in the clear air and one or two in

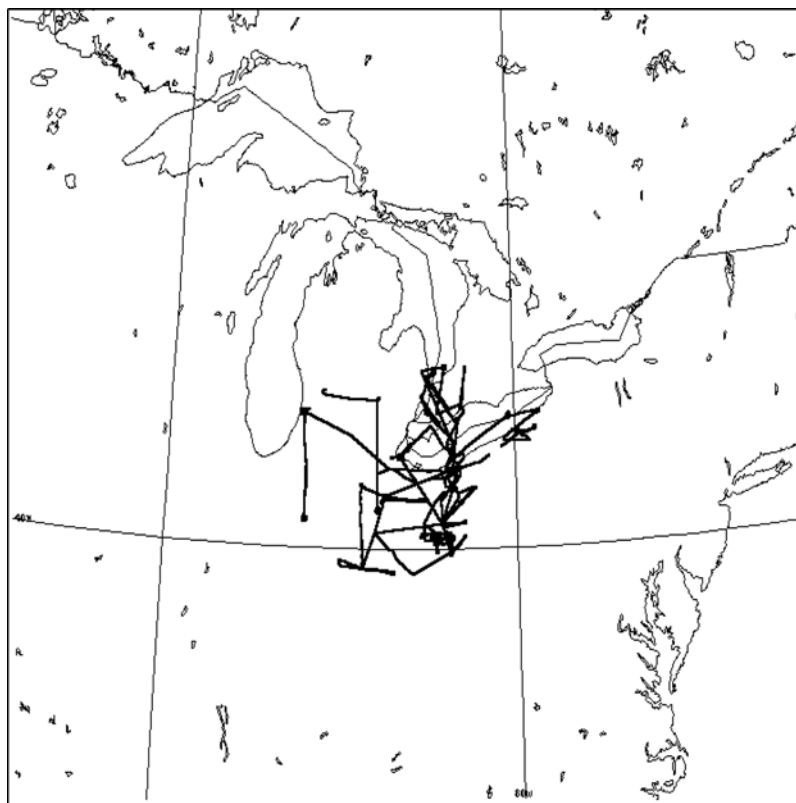


Figure 2. Paths of the 10 selected flights conducted by the Canadian Convair 580 aircraft during the ICARTT campaign.

Table 1. Flight Number, Date, and Time for the Five SCu and Five TCu Cases

Flight Number	Date	Time, UTC
<i>SCu</i>		
F11	3 Aug 2004	1457–1829
F16	10 Aug 2004	1623–2015
F17	10 Aug 2004	2122–0053
F18	11 Aug 2004	1828–2143
F19	12 Aug 2004	1739–2120
<i>TCu</i>		
F12	3 Aug 2004	2025–0009
F13	5 Aug 2004	1623–2102
F14	6 Aug 2004	1618–2037
F20	13 Aug 2004	1915–2323
F21	16 Aug 2004	1846–2155

cloud. Five flights were in TCu, which focused on one (or one cluster of) cumulus with multiple cloud penetrations at different levels. Table 1 lists the flight number, date and time, and type of cloud observed by these flights. GEM simulations covering each flight period were conducted at both horizontal resolutions (15- and 2.5-km) and results were outputted every 15 min. The GEM at 15-km resolution was run for 36 hours with the first 12 hours as spin-up starting at 1200 UTC of the previous day. Hourly output from the 15-km resolution model simulation was used to drive the GEM at 2.5-km resolution for a 24-hour simulation starting at 0000 UTC each day.

[12] Since the ICARTT campaign was conducted during summer time and the Canadian Convair 580 mainly sampled low-level clouds (<3500 m), only warm clouds are considered in this study. LWC was measured with a PMS King probe [King *et al.*, 1978] and with a Nevzorov LWC probes [Korolev *et al.*, 1998; Strapp *et al.*, 2003]. The LWC measurements were averaged at 1-s intervals, representing a horizontal length of 90–100 m. The two LWC probes usually have an agreement within 10% and the detection limit of LWC is about 0.01 g/m^3 . The clouds are assumed to be fully resolved at this resolution and the measured LWC is considered as in-cloud value.

[13] During ICARTT, the observed clouds were mostly scattered in nature and the Convair flight patterns were designed to study chemical transformation and transport processes rather than to make detailed examinations of the cloud fields. It is therefore necessary to devise methodologies to make use of these in situ measurements for the evaluation. In this study, two statistical approaches are applied. One is based on a point-by-point comparison of the modeled and the in situ observed temperature, specific humidity and cloud LWC along flight track following the method used by some of the past model evaluations with in situ aircraft observations [e.g., Guan *et al.*, 2002; Vaillancourt *et al.*, 2003]. As will be shown, the point-by-point comparison for cloud LWC is problematic for the current cases because of the types of clouds sampled, particularly TCus. Even for SCu, unless the individual cloud cells are more densely packed, there is inevitable spatial and temporal mismatch between the model simulations and aircraft observations due to the significant inhomogeneity in the cloud fields, which makes the point-by-point statistical comparison less meaningful. Therefore the main focus of the point-by-point approach (section 3.1) is on the state

parameters (temperature and humidity). For evaluating the modeled LWC with the aircraft observations, the model predicted LWC is compared with the aircraft measurements using a statistical approach over a subdomain that covers individual flight track (section 3.2).

3.1. Statistics Along Flight Tracks

[14] To compare model simulation with aircraft observation along the flight track, the model output at 15 min intervals is numerically interpolated to the 4-D (3-D spatial + 1-D temporal) aircraft in situ locations.

[15] Following the approach taken by Vaillancourt *et al.* [2003], comparison statistics for temperature, specific humidity, and LWC along the flight tracks are summarized in Table 2, for the 15-km resolution model runs, and in Table 3, for the 2.5-km resolution model runs.

[16] Vaillancourt *et al.* [2003] stated that a point-by-point comparison of the aircraft measurement and model simulation is a very severe test given the temporal and spatial mismatch between model simulation and aircraft observation, especially for summer or convective weather conditions (as the cases studied here). Nevertheless, at both resolutions the simulated temperature and specific humidity correlate well with the observations for almost all the cases as seen from the correlation coefficients in Table 2 and 3, independent of cloud types (SCu and TCu). The good correlation of temperature and specific humidity is comparable to what Vaillancourt *et al.* [2003] found in the case of large-scale winter frontal cloud systems.

[17] On the other hand, as expected the comparison of LWC is very poor: only two of the 10 flights (flights 16 and 20) showed even a marginal correlation between the modeled and the observed LWC. This contrasts with the strong positive correlations between modeled and aircraft observed total water content found in the majority of the flights sampling winter frontal clouds in Vaillancourt *et al.* [2003]. The difference is a result of the mismatch between model and aircraft observation in highly inhomogeneous cloud fields as discussed above. To illustrate this, time series of the observed and the modeled LWC along the flight track for two flights (flights 11 and 16) are plotted in Figure 3. The GOES visible channel images corresponding to the time of the flights are shown in Figure 4. For flight 16, the aircraft sampled an area of wide spread SCu ahead of an advancing cold front (Figure 4b). As seen from the aircraft time series, the cloud cells are more packed (Figure 3b). By comparing modeled cloud fields with GOES observation (not shown), it is indicated that the model is able to capture the frontal cloud band well at both resolutions in terms of timing and location, resulting in reasonably good correlation of LWC between the model and the observation. The correlation coefficients between the aircraft observations and the model simulations are 0.38 and 0.33 for the 15- and 2.5-km resolutions, respectively (see Tables 2 and 3). These numbers are comparable to the correlation coefficients given by Vaillancourt *et al.* [2003] for their more successful cases. In contrast, in the case of flight 11, the aircraft sampled a narrow postfrontal SCu band between Lake Erie and Lake Huron (Figure 4a). The aircraft time series indicates more scattered clouds (Figure 3a). This is a situation where the mismatch between the modeled cloud and real cloud is more probable. Indeed

Table 2. Along-the-Track Statistics of Temperature, Specific Humidity, and LWC for the Model at 15 km Resolution^a

	SCu					TCu				
	F11	F16	F17	F18	F19	F12	F13	F14	F20	F21
	<i>Temperature, °C</i>									
Correlation	0.93	0.94	0.96	0.99	0.97	0.99	0.97	0.99	0.99	0.99
Model mean	15.8	11.3	11.5	8.6	7.8	15.6	6.3	9.8	4.9	9.9
Observed mean	15.7	9.6	10.0	7.6	6.7	14.1	6.0	9.1	3.5	8.6
Bias	0.1	1.7	1.5	1.0	1.1	1.5	0.3	0.7	1.4	1.3
Mean absolute error	1.0	1.8	1.7	1.2	1.3	1.6	0.7	0.8	1.4	1.3
Sample number	9911	11713	10812	9911	12485	11712	11039	13515	12614	9010
	<i>Specific Humidity, g/kg</i>									
Correlation	0.81	0.94	0.91	0.81	0.97	0.85	0.65	0.71	0.71	0.79
Model mean	10.3	8.1	8.4	6.4	6.3	9.5	5.0	5.8	6.1	7.2
Observed mean	11.0	8.0	8.0	6.9	6.2	10.7	5.7	6.0	5.7	6.9
Bias	-0.7	0.1	0.4	-0.5	0.1	-1.2	-0.7	-0.2	0.4	0.3
Mean absolute error	1.4	0.5	0.6	0.9	0.5	1.7	1.5	0.7	0.6	0.9
Sample number	9911	11713	10812	9911	12485	11712	11039	13515	12614	9010
	<i>LWC, g/m³</i>									
Correlation	0.17	0.38	0.17	-0.03	0.10	-0.03	0.11	0.00	0.32	0.03
Model mean	0.01	0.02	0.04	0.01	0.004	0.002	0.02	0.00	0.06	0.03
Observed mean	0.02	0.07	0.03	0.03	0.04	0.02	0.04	0.01	0.09	0.03
Bias	-0.01	-0.05	0.01	-0.02	-0.04	-0.02	-0.02	-0.01	-0.03	0.00
Mean absolute error	0.03	0.07	0.05	0.01	0.04	0.02	0.05	0.01	0.10	0.05
Sample number	9911	11713	10812	9911	12485	11712	11039	13515	12614	9010
Number in model	1318	2496	3333	720	1268	450	1787	0	7067	2763
Number in observation	1199	3301	1782	1427	1921	1039	1266	603	3150	1116

^aModel mean and observed mean are computed from all the data points. The bias is defined as the model mean minus the observed mean. Mean absolute error is the mean of the absolute difference between the modeled and observed values along the flight track. Sample number is the total number of data point along flight track. “Number in models” and “Number in observations” are the number of data point with LWC values exceeding 0.01 g m⁻³.

the model at 2.5-km resolution predicted very little cloud along the flight track, and the 15-km resolution model predicted clouds at different locations compared to the observations.

[18] Because of the high temporal and spatial variations of clouds and the relatively low spatial coverage of flight

tracks, it is unrealistic to expect a quantitative one-to-one comparison (in space and time) between the model simulations (at current resolutions) and the aircraft observations of summer convective clouds. The broader statistical approach discussed in the following section provides a

Table 3. Same as Table 2 but for the Model at 2.5 km Resolution

	SCu					TCu				
	F11	F16	F17	F18	F19	F12	F13	F14	F20	F21
	<i>Temperature, °C</i>									
Correlation	0.89	0.95	0.96	0.99	0.97	0.98	0.96	0.99	0.99	0.99
Model mean	15.5	10.5	10.9	8.1	7.5	15.4	6.5	9.5	5.1	10.0
Observed mean	15.7	9.6	10.0	7.6	6.7	14.1	6.0	9.1	3.5	8.6
Bias	-0.2	0.9	0.9	0.5	0.8	1.3	0.5	0.4	1.6	1.4
Mean absolute error	1.5	1.1	1.1	0.7	1.1	2.0	0.9	0.6	1.6	1.5
Sample number	9911	11713	10812	9911	12485	11712	11039	13515	12614	9011
	<i>Specific Humidity, g/kg</i>									
Correlation	0.81	0.92	0.91	0.72	0.97	0.83	0.60	0.70	0.65	0.77
Model mean	9.1	8.2	8.1	6.3	5.9	8.0	4.3	5.5	6.0	6.9
Observed mean	11.0	8.0	8.0	6.9	6.2	10.7	5.7	6.0	5.7	6.9
Bias	-1.9	0.2	0.1	0.6	-0.3	-2.7	-1.4	-0.5	0.3	0.0
Mean absolute error	2.3	0.6	0.5	1.0	0.5	2.8	1.9	1.0	0.6	0.9
Sample number	9911	11713	10812	9911	12485	11712	11039	13515	12614	9010
	<i>LWC, g/m³</i>									
Correlation	-0.02	0.33	-0.03	-0.04	0.12	-0.02	0.01	-0.01	0.29	0.00
Model mean	0.001	0.042	0.008	0.007	0.005	0.002	0.002	0.0002	0.056	0.000
Observed mean	0.020	0.070	0.031	0.025	0.037	0.020	0.036	0.013	0.090	0.032
Bias	-0.019	-0.028	-0.023	-0.018	-0.032	-0.018	-0.034	-0.013	-0.034	-0.032
Mean absolute error	0.030	0.078	0.038	0.032	0.038	0.024	0.038	0.013	0.099	0.032
Sample number	9911	11713	10812	9911	12485	11712	11039	13515	12614	9011
Number in model	70	2690	774	429	469	254	203	31	3310	0
Number in observation	1199	3301	1782	1427	1921	1039	1266	603	3150	1116

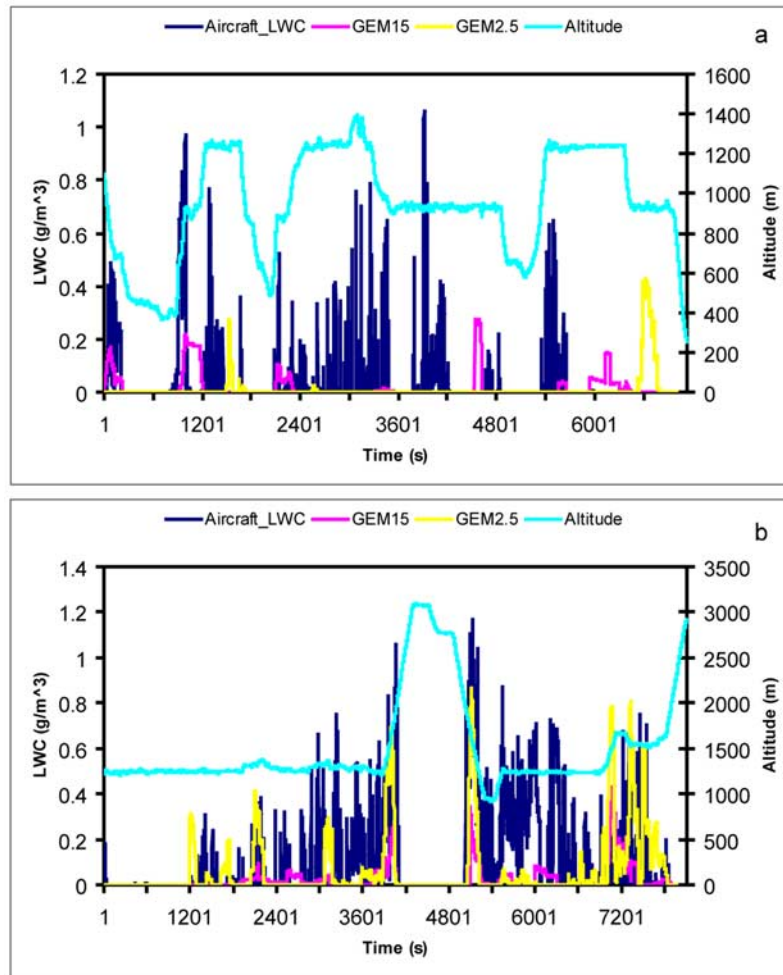


Figure 3. Time series of aircraft observed (blue) and model simulated (pink, 15 km GEM; yellow, 2.5 km GEM) LWC and aircraft altitude (cyan) for the cloudy segment of (a) flight 11 and (b) flight 16.

better test of the model’s ability to predict clouds with similar characteristics.

3.2. Statistics Over Flight Subdomains

[19] For this approach, we assume that the clouds sampled by the aircraft are representative of the clouds in the same area at the same time in terms of microphysical characteristics. This permits the observed LWC along the flight paths to be compared statistically with the model simulated LWC over a 3-D subdomain that covers individual aircraft track during the sampling period (see, for example, the area outlined by the box in Figure 4a for flight 11). In this section the observation statistics are calculated from all 1-s samples with LWC greater than the detection limit 0.01 g m^{-3} , and the model statistics are calculated from all the model grids with LWC greater than 0.01 g m^{-3} within the 3-D subdomains. The model predicted LWCs are at the model grid scale, i.e., 15 km or 2.5 km. As mentioned earlier, the explicit microphysics scheme used for the simulations at 2.5-km resolution does not consider sub-grid-scale cloud, while the Sundqvist condensation scheme, used for the simulations at 15 km resolution, does consider fractional cloud cover at a given grid. Therefore for the 15-km resolution model simulations, both the direct model

prediction of grid-scale LWC (an average between the cloudy and clear-air portions of the grid when cloud fraction is smaller than 1), and the “in-cloud” LWC (diagnosed from the modeled grid-scale LWC divided by the modeled cloud fraction, i.e., LWC in the cloudy portion of the grid) are compared with the observed LWC. Comparisons are made first on the vertical distribution of the cloud LWC and then on the frequency distribution of the LWC. There is a scale compatibility issue when comparing the in situ observation with the model at 2.5- and 15-km resolutions. In principal, one can average the aircraft time series over a sufficient time interval to obtain similar spatial resolution as the model over sufficiently long segments of level flight. This is done for the comparison discussed in section 3.2.3 for the SCu flights. For the TCu flights however, the aircraft mainly focused on individual TCu or a cluster of TCus over a limited horizontal range. In this case averaging the aircraft time series over longer time interval does not translate to a larger spatial representation.

3.2.1. Vertical Distribution

[20] For this comparison, the vertical coordinate is disaggregated into seven bins corresponding to the aircraft sampling levels. The median, 25th and 75th percentiles of

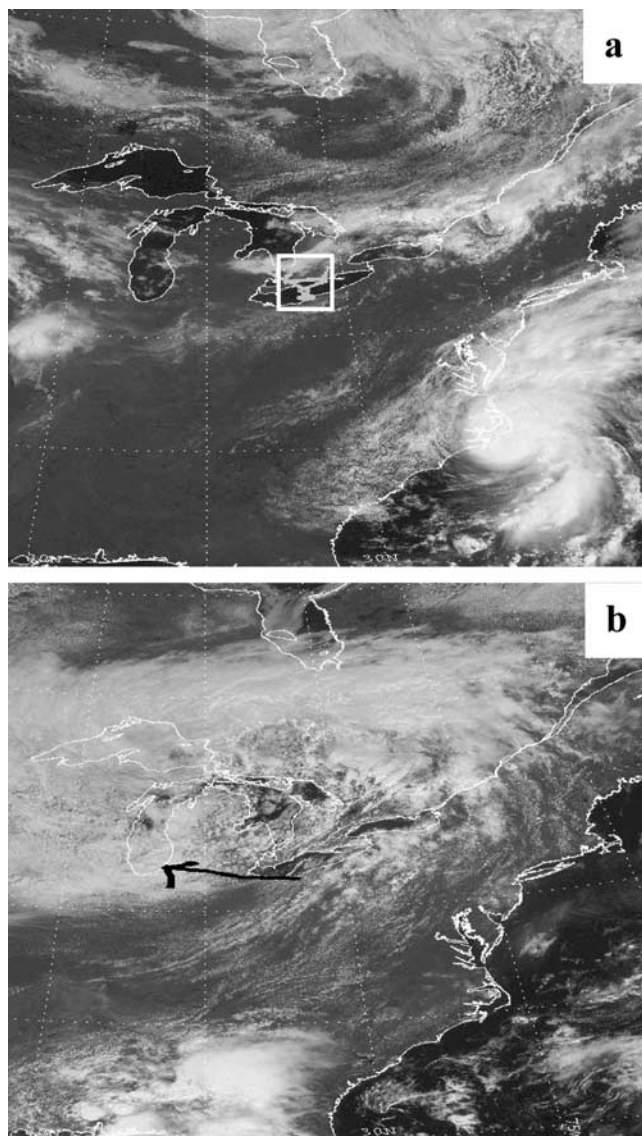


Figure 4. GOES satellite visible channel 1 image over the 15 km horizontal resolution domain (a) at 1515 UTC on 3 August 2004, roughly corresponding to the beginning of flight 11. The gray thick line in the white box is the aircraft flight track, and the white box indicates the subdomain selected for the statistical analysis discussed in section 3.2. (b) At 1645 UTC on 10 August 2004, roughly corresponding to the beginning of flight 16. The black thick line denotes the aircraft flight track.

LWC in each of these altitude bins are calculated for the aircraft observations and the model simulations separately.

[21] For the TCu cases, comparisons are shown in Figure 5. A nearly linear increase in LWC with height within these clouds was observed. This feature was in general reproduced by the model at both horizontal resolutions. In comparison, the model at 2.5-km resolution predicted larger cloud LWC at lower levels and slightly lower LWC at the highest level. The model at 15-km resolution, however, predicted significantly lower LWC at higher levels above 1500 m. It also predicted a slightly higher cloud base in this case (no cloud was predicted at the

lowest 1250 m level). It is not surprising to see the underprediction of grid-scale LWC compared to the aircraft 1-s observations. At 15-km resolution, the TCus are not expected to be resolved at the grid scale. The grid LWC predicted by the model in these cases would be a representation of subgrid-scale cloud condensation averaged over the grid scale. An “in-cloud” LWC can be obtained by dividing the modeled grid-scale LWC by the modeled cloud fraction. Figure 6 repeats the comparison in Figure 5b except for replacing the modeled grid-scale LWC with the diagnosed in-cloud LWC. The model now agrees well at the intermediate levels and overpredicts at the higher levels.

[22] Figure 7 shows the comparison for the SCu flights. Overall the observed LWC are smaller than in the case of the TCu and the variation in the vertical is inconsistent compared with the TCu measurements. The latter may be partly due to the limited sampling levels from the individual SCu flights and the apparently varied levels where the SCu decks were found from flight to flight. The model simulations at 2.5-km resolution again predicted larger LWC values than observed at almost all levels, while the model at 15-km resolution predicted LWC more comparable with the observations. Similarly, Figure 8 compares the model diagnosed “in-cloud” LWC (from the 15-km runs) with the aircraft observations for these SCu flights, and in this case the LWC is significantly overpredicted by the model. However, it needs to be pointed out that this model diagnosed “in-cloud” LWCs do depend on both the grid-scale LWCs and the cloud fractions predicted by the model. Because of the division (by modeled cloud fraction), the level of uncertainty in the diagnosed “in-cloud” LWCs will increase as the cloud fraction gets smaller.

[23] The vertical distribution comparisons also show that there are greater differences between the model and aircraft LWC are often found at the cloud base and top regardless model resolutions, especially for the TCus. This could indicate discrepancies between the modeled and the observed cloud base and top. For example, Figure 5b seems to imply a somewhat higher cloud base from the model at 15-km resolution compared to the measurement. This may also be impacted by the fact that the aircraft sampling at these lower and upper levels were limited to resolve precisely the locations of cloud base and top.

3.2.2. Frequency Distribution of LWC

[24] Frequency distributions of LWC were prepared from the observations and the simulations. For each flight the 1-s in situ LWC measurements along the flight track and the modeled LWC over the subdomain covering the individual flight track are tallied into 16 LWC bins separately to generate the frequency (probability) distributions. They are compared in Figure 9a for all the SCu flights and Figure 9b for the TCu flights. All the data points larger than 1.5 g m^{-3} are binned to the last bin (1.6 g m^{-3}) in these two figures.

[25] Comparing Figures 9a and 9b, it is evident that the occurrence of observed $\text{LWC} > 1 \text{ g m}^{-3}$ is greater for the TCu than the SCu. The frequency of lower LWC was greater for the SCu than for the TCu. LWC values in more convective clouds are usually larger because of the greater depth of these clouds as a result of stronger updrafts [Cotton and Anthes, 1989].

[26] The model at 15-km resolution reproduces the observed frequency distributions at the larger LWC bins

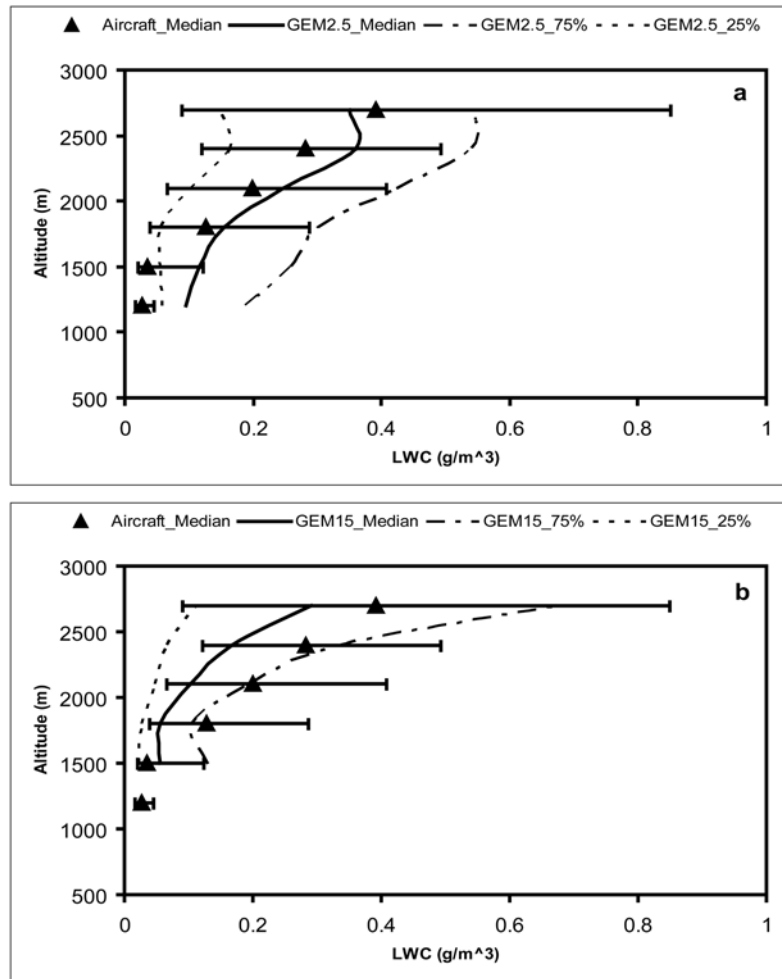


Figure 5. Vertical profiles of modeled and observed median, 25th and 75th percentile of LWC at 7 levels for the 5 TCu cases: (a) model simulation at 2.5-km horizontal resolutions compared with observation and (b) model simulation at 15-km horizontal resolution compared with observation. The triangles mark the median values of the observed LWC, and the error bars are the observed LWC 25th and 75th percentiles. Solid lines are the modeled median LWCs, and dotted and dashed-dotted lines are modeled 25th and 75th percentiles of LWCs.

well, showing a higher frequency for larger LWC in the case of TCu than the case of SCu clouds. However, it also predicts a significantly higher frequency of the lowest LWC bin (0.1 g m^{-3} bin) for TCu than observed. Necessarily, the frequency over the intermediate LWC bins (0.4 to 0.8 g m^{-3}) is lower for the TCu. This is consistent with the underprediction (of grid-scale LWC) found in the vertical comparison. Overall, the frequency distribution of SCu LWC derived from model at 15 km is comparable with the observations and is consistent with the vertical comparisons.

[27] At 2.5-km resolution, there is no significant difference in the predicted LWC frequency distributions between the SCu and TCu flights over the lower LWC bins. However, the model predicts slightly higher frequency over the intermediate LWC bins (between 0.4 and 0.6 g m^{-3}) for the TCu cases. Compared with the observations, the model underpredicts the frequency at the lowest LWC bin and overpredicts the frequency over the intermediate LWC bins for both the SCu and the TCu. Therefore it results in an

overall overprediction of LWC, which is also consistent with the findings from the vertical distribution comparisons.

[28] Figure 10 presents the statistical comparisons in terms of mean, median, 25th and 75th percentiles for all individual flights. The freeform lines on these figures trace the median values of LWC. The difference between the 25th and the 75th percentiles provides a measure of the spread (or range) of the LWC variations.

[29] Although the model at 2.5-km resolution overpredicts LWC for all the flights studied here, the variations of the modeled median and mean are similar from flight to flight to the observed variations, especially for the SCu cases (Figure 10a). Similarly, at 15-km resolution the model is also able to capture the observed variation in LWC from flight to flight. For the SCu cases, the modeled mean and median are comparable with the observations (Figure 10a), while for the TCu case, the 15-km model underpredicts (Figure 10b).

[30] Table 4 summarizes the mean and standard deviation of LWC from both the observations and the model simu-

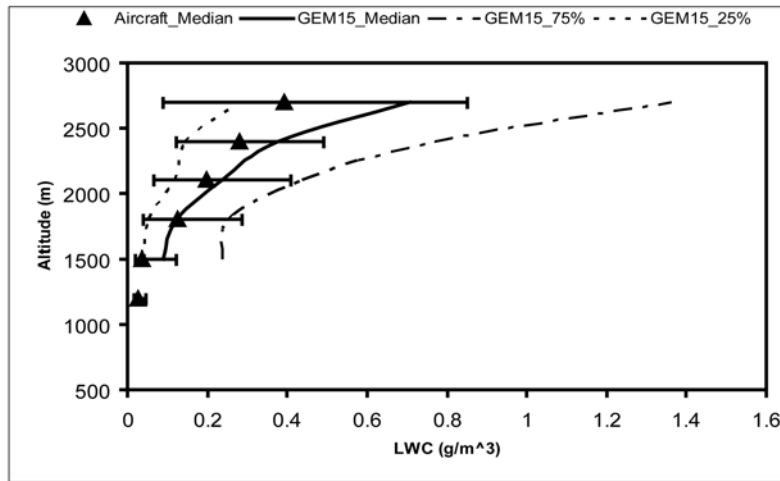


Figure 6. Same as Figure 5b but for the calculated “in-cloud” LWC values from the model simulation at 15-km horizontal resolution.

lations for all the SCu and TCu flights. Both the observations and the model simulations (at both resolutions) show higher mean and standard deviation for the TCu cases than for the SCu cases. Again, it is seen that the model at 2.5 km

resolution overpredicts the mean LWC, by 45% and 24% for the SCu and TCUs, respectively, but the model-predicted standard deviations are comparable to those from the observations. At 15-km resolution, the model underpredicts

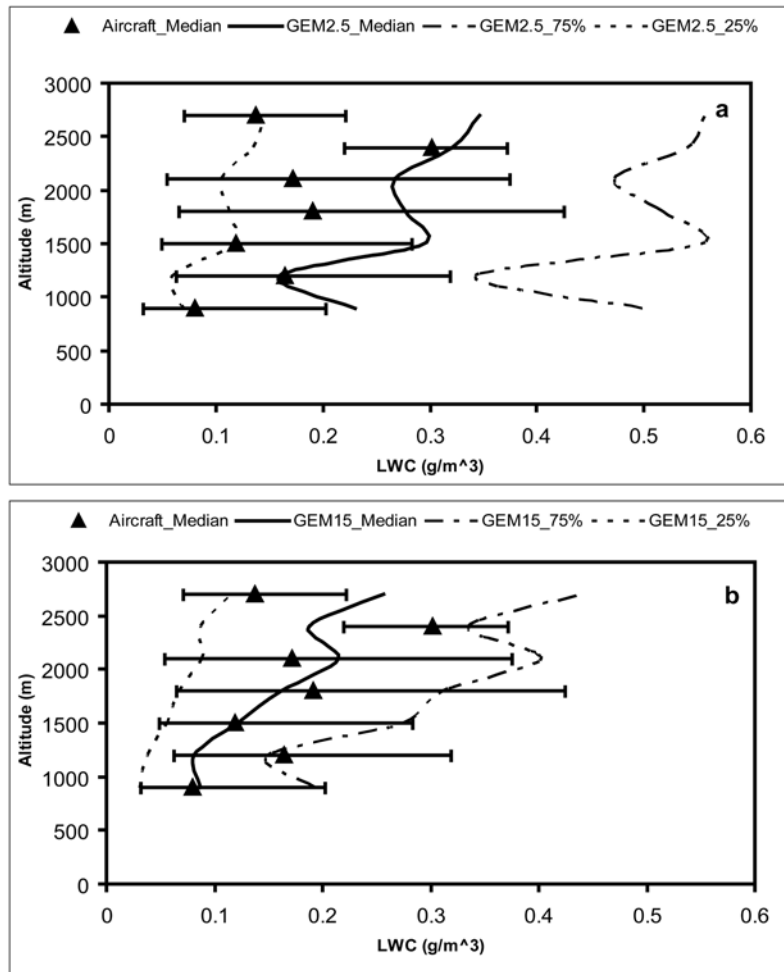


Figure 7. Same as Figure 5 but for the 5 SCu cases: model simulations at (a) 2.5-km and (b) 15-km resolutions compared to observations.

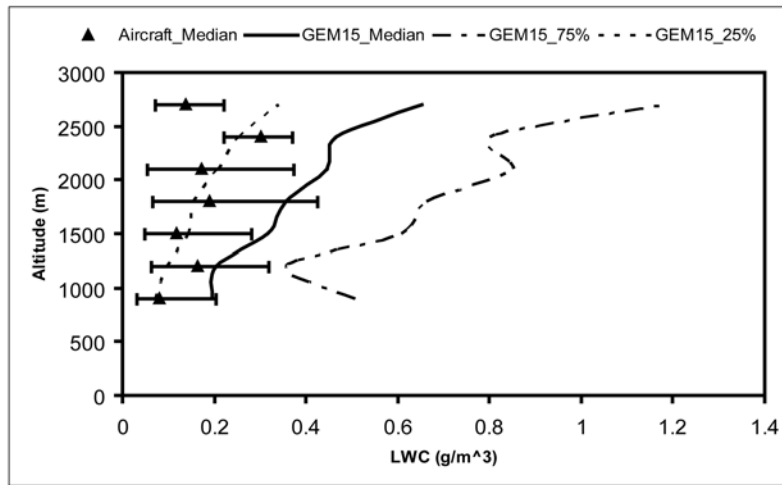


Figure 8. Same as Figure 7b but for the calculated “in-cloud” LWC values at 15-km horizontal resolution.

both the mean and standard deviation. The underpredictions in mean LWC are about 23% and 35% for the SCu and the TCu cases, respectively.

[31] As pointed out in section 3.2.1, the underprediction in grid-scale LWC by the model at 15-km resolution is

expected because of the difference in spatial scales represented by the model, 15 km, and aircraft measurement (1-s, or approximately 100 m). For all the cases studied here (SCu and TCu) the observed clouds are at much smaller scale than the model scale (15 km). In fact, the mean cloud

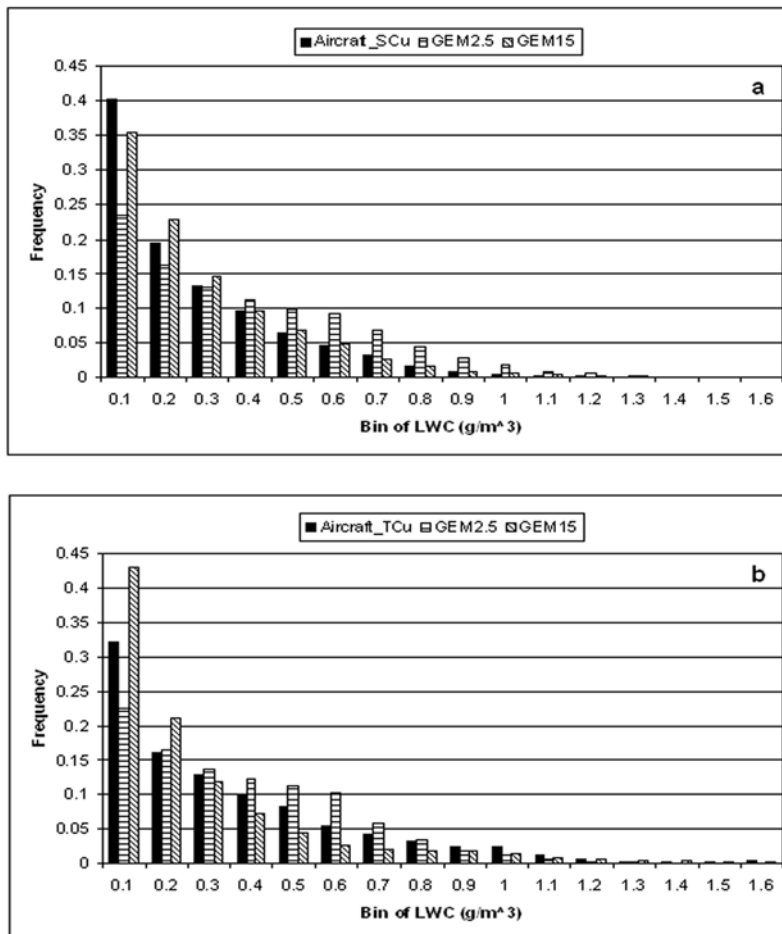


Figure 9. Comparison of frequency distributions of LWC for the (a) 5 SCu and (b) 5 TCu flights.

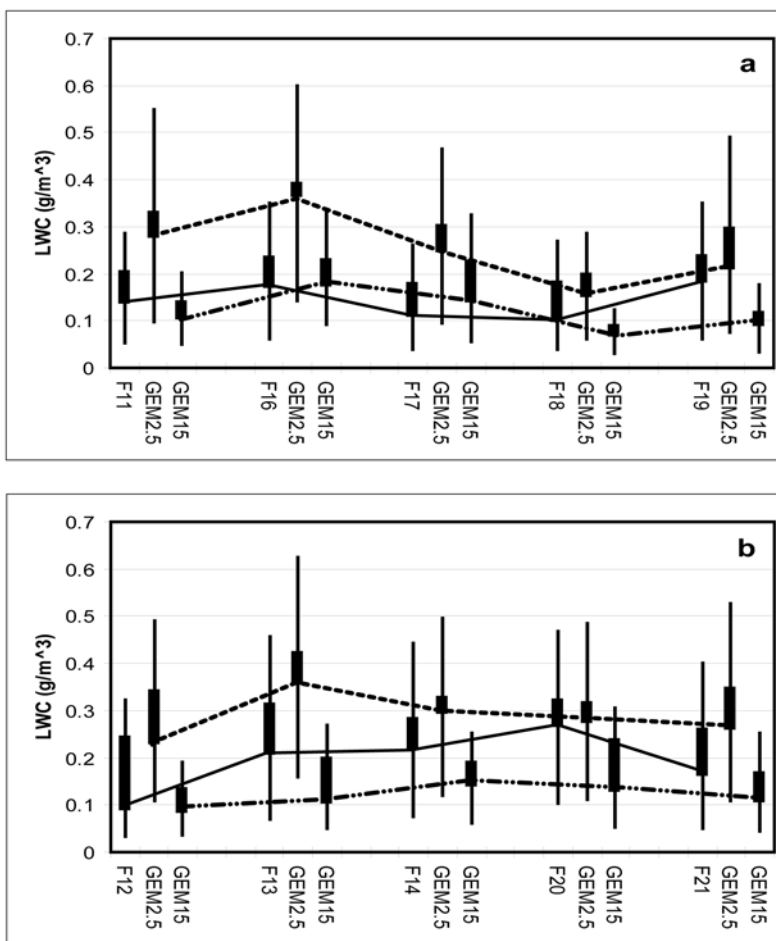


Figure 10. Comparison of the observed and modeled LWC statistics: 25th percentile (bottom of the vertical lines), median (bottom of the bars), mean (top of the bars), and 75th percentile (top of the vertical lines) for the (a) 5 SCu flights and (b) 5 TCu flights. Freeform lines trace the median values of LWC.

fractions predicted by the 15-km model simulations for all the cloudy grids are smaller than 50% for all of the 10 cases. The grid-scale LWC is converted to the in-cloud LWC, i.e., LWC in the cloudy portion of the grid, using the modeled cloud fraction as in section 3.2.1. Figure 11 shows the similar plots as in Figure 10 but compares both the grid-scale and the “in-cloud” LWC from the model simulation at 15 km resolution with the observations. The model significantly overpredicts the in-cloud LWCs, by about 99% and 74% in terms of mean LWC (Table 4) for the SCu and the TCu cases, respectively. However, the range between the median and mean values of the modeled “in-cloud” LWC can be very large for some flights (flights 13, 17, and 20). These are the cases where the modeled mean “in-cloud”

LWC is strongly influenced by a few data points with unrealistically large LWC values, which in turn are often driven by the small modeled cloud fractions at some grid points.

[32] It is relevant to air quality modeling to assess how a model performs in predicting the “in-cloud” LWC. For example, *Gong et al.* [2006a] considered fractional cloud cover for the cloud processing of gases and aerosols in the regional air quality model AURAMS. For a given cloudy grid the cloud processing (scavenging of aerosol particles, condensation of soluble gases on cloud droplets, and aqueous phase oxidation) is carried out for the cloudy portion of the grid only, with the “in-cloud” LWC derived from the modeled grid-scale LWC and modeled cloud

Table 4. Mean and Standard Deviation of LWC Derived From Aircraft Observations and Model Simulations for the Five SCu and Five TCu Cases^a

	Aircraft		GEM2.5		GEM15_Grid		GEM15_In-cloud	
	Mean	STD	Mean	STD	Mean	STD	Mean	STD
SCu	0.208	0.203	0.304	0.248	0.161	0.148	0.414	0.456
TCu	0.285	0.291	0.351	0.283	0.185	0.196	0.497	0.644

^aThey are based on, in the case of observation, all sampling points with LWC > 0.01 g m⁻³, and in the case of model, all grid points with LWC > 0.01 g m⁻³. Unit is g m⁻³.

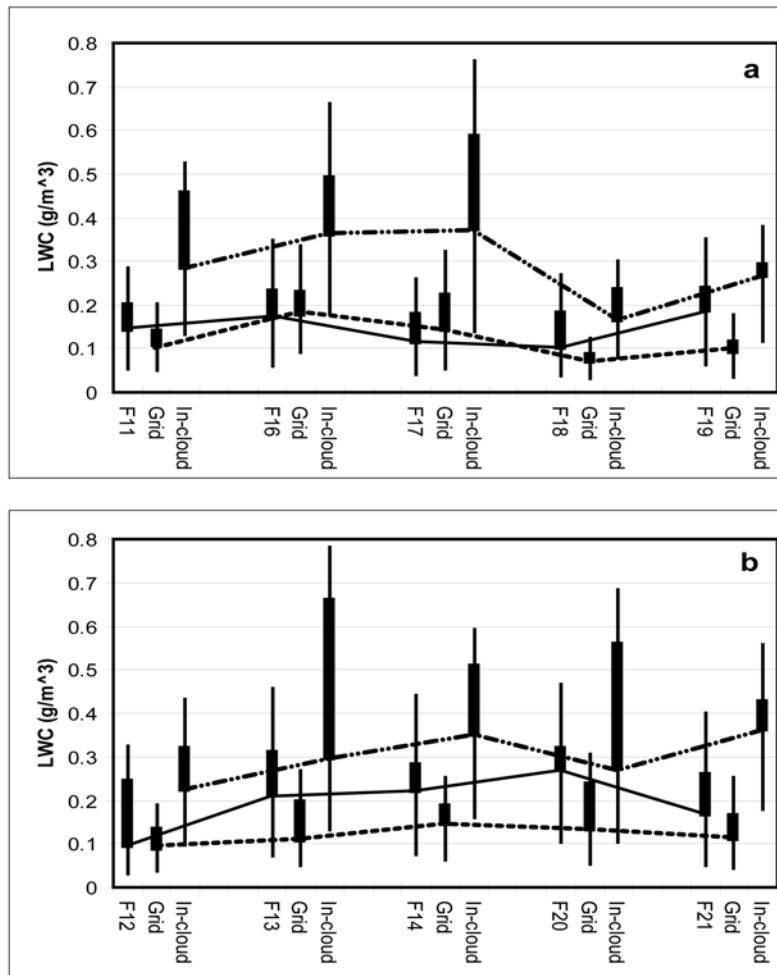


Figure 11. Same as Figure 10 but for comparing both grid and “in-cloud” LWC statistics, from the 15-km resolution simulation, with the in situ observations: (a) 5 SCu flights and (b) 5 TCu flights.

fraction in much the same way as in this study, i.e., grid-scale LWC divided by cloud fraction. The gas and aerosol concentrations at model grid scale are then updated by a weighted average between the cloud-processed and the clear-air gas and aerosol concentrations according to the cloud fraction. As shown here, one needs to be careful about the use of model derived “in-cloud” LWC, particularly when modeled cloud fractions are small. In this study, diagnosed in-cloud LWC from the model at 15-km resolution can exceed 10 g m^{-3} because of small cloud fraction, while very few data points from the in situ observation exceed 1.5 g m^{-3} . For the version of Sundqvist condensation scheme used in the GEM at 15-km resolution, although the parameterization of condensation takes fractional cloudiness into account, the cloud fraction is determined from relative humidity and a threshold relative humidity above which clouds are assumed to form within a grid box. The thresholds of relative humidity are predefined [Sundqvist *et al.*, 1989]. Therefore significant uncertainty exists in the modeled cloud fraction, which will in turn affect the calculated “in-cloud” LWC.

3.2.3. Comparison at Model Grid Scale

[33] So far, the model’s performance in predicting cloud LWC has been evaluated through comparison of the mod-

eled grid-scale and so-called “in-cloud” values with the aircraft 1-s in situ measurements. As mentioned earlier, there is a significant discrepancy in spatial scales between the model and the observation. The model derived “in-cloud” LWC from the simulation at 15-km resolution suffers from significant uncertainties when the subgrid cloud fractions are small. Here, the measurements are scaled up to the model grid sizes so that the comparison between the model simulations and the observations can be made with better scale compatibility. To do this, running averages of the aircraft 1-s time series are carried out over a time interval corresponding to the spatial distance of 2.5- and 15-km (or 25-s and 150-s, respectively). This can only be done meaningfully over the horizontal flight legs that extend at least several grid lengths and, therefore, limits the comparison to the SCu flights only. The TCu flights mainly focused on individual clouds or cluster of clouds with insufficient horizontal coverage to warrant such comparison, particularly for the grid scale at 15-km.

[34] Figure 12 shows the similar comparisons as in Figure 10 but at the model scales here. Specifically, Figure 12a shows the model-observation comparison at 15-km resolution, while Figure 12b shows the comparison at 2.5-km resolution. First of all, we can see that overall the

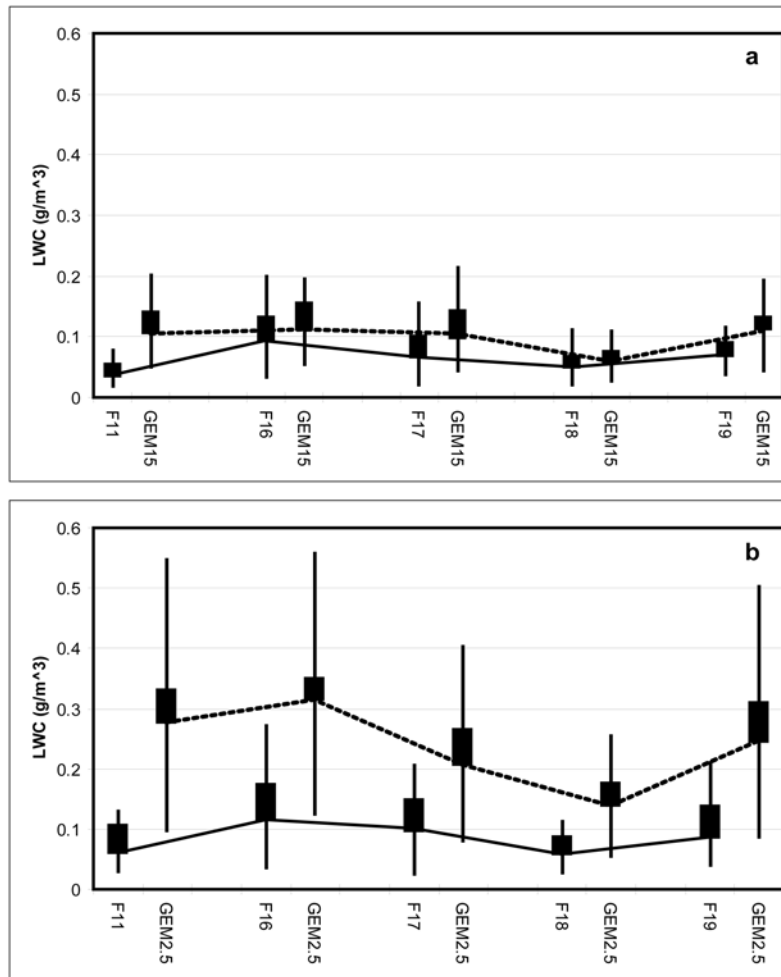


Figure 12. Comparison of modeled and observed LWC statistics at model grid scales for the SCu cases: 25th percentile (bottom of the vertical lines), median (bottom of the bars), mean (top of the bars), and 75th percentile (top of the vertical lines) (a) at 15 km grid scale and (b) at 2.5 km grid scale. Freeform lines trace the median values of LWC.

observed LWC scaled up to 15 km is smaller than that to 2.5 km (e.g., the mean LWC over all 5 flights is 0.09 g m^{-3} at 15 km versus 0.13 g m^{-3} at 2.5 km). It reflects the fact that the clouds studied here are scattered in nature with horizontal dimensions much smaller than 15 km (or even smaller than 2.5 km, see discussion below). The longer distance over which the observational data is averaged, the more clear-air data points are included resulting in smaller mean value. Note that the analysis excludes all clear-air segments. In general the comparison at 15-km resolution is good: the model and the observation follow each other reasonably well in the variation from flight to flight with similar frequency distributions (shapes) as indicated by the differences between, for example, mean and median, the 75th and the 25th percentiles. However, the model overpredicts the LWC by 46% in terms of the mean values (i.e., observation at 0.09 versus model at 0.13). There is a larger overprediction in the simulations at 2.5 km compared to the observations at the same scale. The overprediction in mean LWC is 120% (observation at 0.13 versus model at 0.29). This is discussed again later. Despite the overprediction, the

model results and the observations again show similar variation from flight to flight.

[35] Histograms of the LWC frequency distributions at 15- and 2.5-km grid scales are shown in Figures 13a and 13b, respectively. The comparison at 15-km resolution shows that the model predicts a somewhat lower frequency than the observation at the smallest LWC bin (0.1 g m^{-3}), but overpredicts the frequency over the intermediate and higher LWC bins. At the 2.5-km resolution the model also underpredicts over smaller LWC bins and overpredicts over larger LWC bins but much more significantly compared to the model simulation at 15-km resolution. It needs to be pointed out that, while the Sundqvist condensation scheme used in the 15-km resolution model simulation does allow condensation at subgrid scale (i.e., condensation will start at relative humidity smaller than 100% at grid scale), the explicit Kong-Yau microphysics scheme used in the 2.5-km resolution model simulation does not consider fractional cloud cover (i.e., condensation will only occur when saturation is reached at grid scale). Also included in Figure 13b is the frequency distribution from the aircraft measurement applying the same running mean procedure as previously

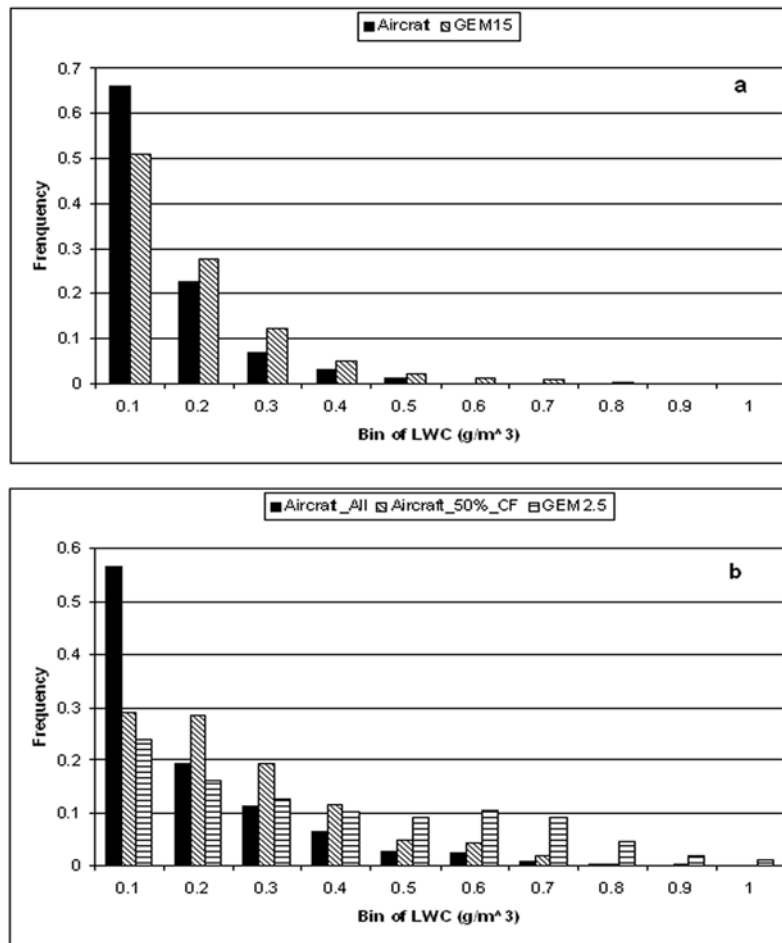


Figure 13. Comparison of modeled and observed frequency distributions of LWC at model grid scales for the 5 SCu flights: (a) 15-km resolution model simulation versus in situ observations averaged over 150-s segments (equivalent to 15 km) and (b) 2.5-km model simulation versus in situ observations averaged over 25-s segments (2.5 km). Also included in Figure 13b is the frequency distribution from the in situ LWC observations averaged over 25-s segments but excluding the ones with more than 50% sampling points in clear air (denoted as Aircraft_50%_CF).

(i.e., over 25-s segments) but excluding the segments with more than 50% sampling points in clear air, (i.e., excluding the cloud cells with a much smaller dimension than 2.5 km). As seen, the frequency over the smallest LWC bin decreased considerably from the measurement, indicating that the low-LWC observations at 2.5-km resolution were influenced significantly by the clouds with much smaller dimension than 2.5 km which the model is unable to resolve. With these data points removed from the analysis the model is seen to come significantly closer to the observations, with the overprediction in mean LWC reduced from 120% (see above) to about 40%. However, the model still predicts more frequent occurrences of large LWCs than the observations.

[36] There may be multiple causes why the model overpredicts the LWC in the cases studied here. For example, in the Kong-Yau microphysics scheme, the condensation/evaporation process is parameterized using a saturation adjustment scheme [Kong and Yau, 1997]; that is, moisture is condensed/evaporated to achieve exact saturation (with the allowance for subsaturation if there is insufficient liquid water available to be evaporated). A number of studies [e.g.,

Clark, 1973; Kogan and Martin, 1994] showed that the saturation adjustment scheme might significantly overestimate the condensation rate, which can lead to overprediction of LWC in some situations. By comparing the saturation adjustment scheme with a detailed explicit microphysical scheme, Kogan and Martin [1994] showed that the overestimated condensation rate in the saturation adjustment scheme can lead to a 40% overprediction in marine SCu, with relatively low CCN number concentration ($\sim 50 \text{ cm}^{-3}$) and low updraft velocity ($\sim 1 \text{ m s}^{-1}$ or lower), i.e., a situation when low condensation rate is expected. However, under continental convective situations with moderate to high CCN concentrations and stronger updraft, such as the cases in the present study, the error induced from the saturation adjustment scheme is small. Other processes, such as removing of LWC through autoconversion and accretion, can also be important. On the basis of limited case studies, J. A. Milbrandt (personal communication, 2006) found that a more sophisticated multimoment bulk microphysics parameterization [Milbrandt and Yau, 2005a, 2005b] produced noticeably smaller LWC than Kong-Yau

scheme. This multimoment scheme is being considered as an alternative microphysical scheme for high-resolution GEM simulations. In any case, investigating the possible deficiencies in model parameterization responsible for the model overprediction of LWC compared to observations deserves a separate study that is beyond the scope of this study.

4. Conclusions

[37] To provide a basis for analyzing and evaluating cloud processing of gases and aerosols in air quality models, the performance of a meteorological model (the GEM model) at two horizontal resolutions, 2.5 and 15 km, is evaluated against aircraft observations with a focus on cloud LWC.

[38] The point-by-point statistics along the flight track showed reasonably good correlations between the aircraft observed and the model simulated thermodynamical fields, such as temperature and specific humidity. Almost no correlation was found between the modeled and the observed LWC, independent of cloud types. It indicates significant timing and placement mismatches between the aircraft observations and the model simulations for the fields of more discrete nature. Because of the spatial and temporal disparity, it is difficult to quantitatively compare the model predicted cloud water content at current resolution with aircraft observation on a strictly point-to-point basis, especially for summer convective clouds.

[39] The statistical analysis over subdomains covering the individual flight tracks showed that the model in general captured the observed vertical distribution of LWC in the TCu. The model also reproduced the observed variation in the LWC statistics among different flights. The model at both resolutions overpredicted the “in-cloud” LWC but the agreement with the observed LWC is closer for the 2.5-km resolution (Table 4). When the model-observation comparison is done at grid scales (for the SCu flights only), the model at 15-km resolution performs better than the model at 2.5-km resolution, although again the model overpredicts the mean LWC at both resolutions. The poorer performance of the model at 2.5 km resolution in this case is mainly due to the inability of the microphysics scheme to represent subgrid-scale clouds, which led to the underprediction of the occurrence of low LWC ($<0.1 \text{ g m}^{-3}$) as seen in Figure 13b. It suggests that for the clouds studied here, one needs to either run model at a much higher resolution than 2.5 km with the current Kong-Yau explicit scheme or enhance the scheme so that it can consider subgrid-scale condensation. However, these clouds with low LWCs are generally not as important for in-cloud oxidation.

[40] The overestimation of LWC by meteorological model (the GEM model) seen for the cases studied here will have subsequent impact on the cloud processing of gases and aerosols in our air quality model. This study also raises an issue on how subgrid-scale cloud processing may be best parameterized in air quality model given the uncertainties involved in estimating in-cloud values. These issues will be investigated in our future studies.

[41] **Acknowledgments.** We thank the three anonymous reviewers for their comments for improving the manuscript. We are grateful to Mark Couture for providing the aircraft observational data and to Sylvie Gravel for her help with the GEM model. We would also like to acknowledge

Amin Erfani and Jason Milbrandt for their useful suggestions and our colleagues at ARQI, MSC, for their support. Junhua Zhang is supported by the MSC/NESRC Visiting Fellowship program.

References

- Barth, M. C., P. J. Rasch, J. T. Kiehl, C. M. Benkovitz, and S. E. Schwartz (2000), Sulfur chemistry in the National Center for Atmospheric Research Community Climate Model: Description, evaluation, features, and sensitivity to aqueous chemistry, *J. Geophys. Res.*, *105*, 1387–1415.
- Bélair, S., J. Mailhot, C. Girard, and P. Vaillancourt (2005), Boundary layer and shallow cumulus clouds in a medium-range forecast of a large-scale weather system, *Mon. Weather Rev.*, *133*, 1938–1960.
- Brown, P. R. A., and H. A. Swann (1997), Evaluation of key microphysical parameters in three-dimensional cloud-model simulations using aircraft and multiparameter radar data, *Q. J. R. Meteorol. Soc.*, *123*, 2245–2275.
- Carmichael, G. R., L. K. Peters, and R. D. Saylor (1991), The STEM-II regional scale acid deposition and photochemical oxidant model—I. An overview of model development and applications, *Atmos. Environ., Part A*, *25*, 2077–2090.
- Chang, J. S., R. A. Brost, I. S. A. Isaksen, S. Madronich, P. Middleton, W. R. Stockwell, and C. J. Walcek (1987), A three-dimensional Eulerian acid deposition model: Physical concept and formulation, *J. Geophys. Res.*, *92*, 14,681–14,700.
- Clark, T. L. (1973), Numerical modeling of the dynamics and microphysics of warm cumulus convection, *J. Atmos. Sci.*, *30*, 857–878.
- Clarke, A. D. (1993), Atmospheric nuclei in the Pacific midtroposphere: Their nature, concentration, and evolution, *J. Geophys. Res.*, *98*, 20,633–20,647.
- Côté, J., J.-G. Desmarais, S. Gravel, A. Méthot, A. Patoine, M. Roch, and A. Staniforth (1998a), The operational CMC-MRB Global Environment Multiscale (GEM) model. Part I: Design considerations and formulation, *Mon. Weather Rev.*, *126*, 1373–1395.
- Côté, J., J.-G. Desmarais, S. Gravel, A. Méthot, A. Patoine, M. Roch, and A. Staniforth (1998b), The operational CMC-MRB Global Environmental Multiscale (GEM) Model: Part I—Design considerations and formulation, Part II—Results, *Mon. Weather Rev.*, *126*, 1397–1418.
- Cotton, W. R., and R. A. Anthes (1989), *Storm and Cloud Dynamics*, pp. 5–10, Elsevier, New York.
- Dennis, R. L., J. N. McHenry, W. R. Barchet, F. S. Binkowski, and D. W. Byun (1993), Correcting RADM’s sulphate underprediction: Discovery and correction of model errors and testing the corrections through comparisons against field data, *Atmos. Environ., Part A*, *27*, 975–997.
- Fehsenfeld, F. C., et al. (2006), International Consortium for Atmospheric Research on Transport and Transformation (ICARTT): North America to Europe—Overview of the 2004 summer field study, *J. Geophys. Res.*, *111*, D23S01, doi:10.1029/2006JD007829.
- Garvert, M. F., C. P. Woods, B. A. Colle, C. F. Mass, P. V. Hobbs, M. T. Stoelinga, and J. B. Wolfe (2005), The 13–14 December 2001 IMPROVE-2 event. Part II: Comparison of MM5 model simulations of clouds and precipitation with observations, *J. Atmos. Sci.*, *62*, 3520–3534.
- Gong, W., et al. (2006a), Cloud processing of gases and aerosols in A Regional Air Quality Model (AURAMS), *Atmos. Res.*, *82*, 248–275.
- Gong, W., V. S. Bouchet, P. A. Makar, M. D. Moran, S. Gong, A. P. Dastoor, B. Pabla, and W. R. Leitch (2006b), Cloud processing of gases and aerosols in a regional air quality model (AURAMS): Evaluation against aircraft data, in *Air Pollution Modelling and Its Application XVII*, edited by C. Borrego and A.-L. Norman, pp. 553–561, Springer, New York.
- Guan, H., S. G. Cober, and G. A. Isaac (2001), Verification of supercooled cloud water forecasts with in situ aircraft measurements, *Weather Forecasting*, *16*, 145–155.
- Guan, H., S. G. Cober, G. A. Isaac, A. Tremblay, and A. Méthot (2002), Comparison of three cloud forecast schemes with in situ aircraft measurements, *Weather Forecasting*, *17*, 1226–1235.
- Kain, J. S. (2004), The Kain-Fritsch convective parameterization: An update, *J. Appl. Meteorol.*, *43*, 170–181.
- Kain, J. S., and J. M. Fritsch (1990), A one-dimensional entraining-detraining plume model and its application in convective parameterization, *J. Atmos. Sci.*, *47*, 2784–2802.
- Karamchandani, P., and A. Venkatram (1992), The role of non-precipitating clouds in producing ambient sulphate during summer: Results from simulations with the acid deposition and oxidant model (ADOM), *Atmos. Environ., Part A*, *26*, 1041–1052.
- King, W. D., D. A. Parkin, and R. J. Handsworth (1978), A hot-wire water device having fully calculable response characteristics, *J. Appl. Meteorol.*, *17*, 1809–1813.
- Kogan, Y. L., and W. J. Martin (1994), Parameterization of bulk condensation in numerical cloud models, *J. Atmos. Sci.*, *51*, 1728–1739.
- Kong, F. Y., and M. K. Yau (1997), An explicit approach to microphysics in MC2, *Atmos. Ocean*, *35*, 257–291.

- Korolev, A. V., J. W. Strapp, G. A. Isaac, and A. N. Nevzorov (1998), The Nevzorov airborne hot-wire LWC-TWC probe: Principle of operation and performance characteristics, *J. Atmos. Oceanic Technol.*, *15*, 1495–1510.
- Lohmann, U., K. von Salzen, N. McFarlane, H. G. Leighton, and J. Feichter (1999), Tropospheric sulfur cycle in the Canadian general circulation model, *J. Geophys. Res.*, *104*, 26,833–26,858.
- Mailhot, J., et al. (2006), The 15-km version of the Canadian regional forecast system, *Atmos. Ocean*, *44*, 133–149.
- McHenry, J. N., and R. L. Dennis (1994), The relative importance of oxidation pathways and clouds to atmospheric ambient sulphate production as predicted by the Regional Acid Deposition Model, *J. Appl. Meteorol.*, *33*, 890–905.
- Milbrandt, J. A., and M. K. Yau (2005a), A multimoment bulk microphysics parameterization. Part I: Analysis of the role of the spectral shape parameter, *J. Atmos. Sci.*, *62*, 3051–3064.
- Milbrandt, J. A., and M. K. Yau (2005b), A multimoment bulk microphysics parameterization. Part II: A proposed three-moment closure and scheme description, *J. Atmos. Sci.*, *62*, 3065–3081.
- Moran, M. D., A. P. Dastoor, S.-L. Gong, W. Gong, and P. A. Makar (1998), Conceptual design for the AES unified regional air quality modelling system (AURAMS), internal report, 100 pp., Air Qual. Res. Branch, Meteorol. Serv. of Can., Toronto, Ont., Canada.
- Raes, F., and R. Van Dingenen (1992), Simulations of condensation and cloud condensation nuclei from biogenic SO₂ in the remote marine boundary layer, *J. Geophys. Res.*, *97*, 12,901–12,912.
- Rasch, P. J., M. C. Barth, J. T. Kiehl, S. E. Schwartz, and C. M. Benkovitz (2000), A description of the global sulphur cycle and its controlling processes in the National Center for Atmospheric Research Community Climate Model, Version 3, *J. Geophys. Res.*, *105*, 1367–1385.
- Reisner, J., R. M. Rasmussen, and R. T. Bruintjes (1998), Explicit forecasting of supercooled liquid water in winter storms using the MM5 mesoscale model, *Q. J. R. Meteorol. Soc.*, *124*, 1071–1107.
- Renard, M., N. Chaumerliac, and S. Cautenet (1994), Tracer redistribution by clouds in West Africa: Numerical modeling for dry and wet seasons, *J. Geophys. Res.*, *99*, 12,873–12,883.
- Seinfeld, J. H., and S. N. Pandis (1998), *Atmospheric Chemistry and Physics*, 1326 pp., Wiley-Interscience, Hoboken, N. J.
- Strapp, J. W., J. Oldenburg, R. Ide, L. Lilie, S. Bacic, Z. Vukovic, M. Oleskiw, D. Miller, E. Emery, and G. Leone (2003), Wind tunnel measurements of the response of hot-wire liquid water content instruments to large droplets, *J. Atmos. Oceanic Technol.*, *20*, 791–806.
- Sundqvist, H., E. Berge, and J. E. Krisjansson (1989), Condensation and cloud parameterization studies with a mesoscale numerical weather prediction model, *Mon. Weather Rev.*, *117*, 1641–1657.
- Vaillancourt, P. A., A. Tremblay, S. G. Cober, and G. A. Isaac (2003), Comparison of aircraft observations with mixed-phase cloud simulations, *Mon. Weather Rev.*, *131*, 656–671.
- Venkatram, A., P. K. Karamchandani, and P. K. Misra (1988), Testing a comprehensive acid deposition model, *Atmos. Environ.*, *22*, 737–747.
- von Salzen, K., H. G. Leighton, P. A. Ariya, L. A. Barrie, S. L. Gong, J.-P. Blanchet, L. Spacek, U. Lohmann, and L. I. Kleinman (2000), Sensitivity of sulphate aerosol size distributions and CCN concentrations over North America to SO_x emission and H₂O₂ concentrations, *J. Geophys. Res.*, *105*, 9741–9765.
- Wang, C., and R. G. Prinn (2000), On the roles of deep convective clouds in tropospheric chemistry, *J. Geophys. Res.*, *105*, 22,269–22,297.

W. Gong, W. R. Leitch, J. W. Strapp, and J. Zhang, Science and Technology Branch, Environment Canada, 4905 Dufferin Street, Toronto, ON M3H 5T4, Canada. (junhua.zhang@ec.gc.ca)